8964

Subtidal Response of the Scotian Shelf Bottom Pressure Field to Meteorological Forcing

Franklin B. Schwing[1]
Department of Oceanography, Dalhousie University
Halifax, Nova Scotia B3H 4J1

[Original manuscript received 1 May 1988; in revised form 28 June 1988]

ABSTRACT *Data collected during the Canadian Atlantic Storms Program (CASP) show subtidal variations in subsurface pressure (SSP) to be highly coherent throughout the Scotian Shelf region, and well correlated to fluctuations in the alongshelf component of wind stress (τ^y). Analysis using a frequency-dependent multiple regression model verified that τ^y is the primary source of local forcing to the SSP field, although non-locally generated variations in SSP are also important. The two components of local wind stress and a non-local SSP term combine to explain over 90% of SSP variance on the Scotian Shelf.*

Statistical results describing the response to τ^y change dramatically depending upon the inclusion of non-local forcing. In a model including both types of forcing, the SSP response to local forcing behaves like the solution to a dynamical model forced by time-dependent wind stress with sea-level prescribed to zero at the eastern cross-shelf boundary. Local τ^y forcing becomes more effective to the west and onshore, whereas the phase suggests propagation to the west. The importance of τ^y is reduced at higher frequencies. Describing SSP with a statistical model containing local forcing alone may lead to an incorrect interpretation of SSP dynamics, particularly in the synoptic band where the wind variance is greatest.

Energy originating from a non-local source is most obvious at $\omega > 0.5$ cpd and at locations on the eastern half of the shelf, but plays an important role at all sites and at all frequencies. These variations propagate to the west at speeds of 6.5 ($\omega < 0.2$ cpd), 25–33 (0.2 cpd $< \omega <$ 0.5 cpd), and 12–17m s^{-1} ($\omega > 0.5$ cpd). The exponential decay scales at all frequencies are ~900 km in the direction of phase propagation. The non-local response is consistent with theoretical estimates of first- and second-mode shelf waves for this region and represents the most direct evidence of shelf wave activity on the Scotian Shelf to date.

RÉSUMÉ *Des données récoltées durant le Programme canadien d'étude des tempêtes dans l'Atlantique (PCETA) montrent que les variations infra-tidales de la pression de fond (PF) sont fortement cohérentes dans toute la région du plateau Scotian, et présentent une bonne corrélation avec les fluctuations de la composante de la tension du vent (τ^y) parallèle au plateau. L'analyse par un modèle à régression multiple, dépendant de la fréquence, a vérifié que τ^y est la source primaire de forçage local du champ de la PF, bien que des variations d'origine non locale de la PF soient également importantes. Les deux composantes (tension du vent locale et terme non local de la PF) combinées, rendent compte de plus de 90% de la variance de la PF sur le plateau Scotian.*

[1]Present address: SW Fisheries Center, National Marine Fisheries Service, P.O. Box 831, Monterey, CA 93942, U.S.A.

ATMOSPHERE-OCEAN 27 (1) 1989, 157–180 0705-5900/89/0000-0157$01.25/0
© Canadian Meteorological and Oceanographic Society

Les résultats statistiques décrivant la réaction à τ^y changent dramatiquement si l'on introduit un forçage non local. Dans un modèle incluant les deux types de forçages, la réaction de la PF au forçage local se comporte comme la solution d'un modèle dynamique forcé par une tension du vent dépendante du temps, et où le niveau de la mer est prescrit à zéro à la limite orientale perpendiculaire au plateau. Le forçage local de τ^y devient plus effectif vers l'ouest et vers le rivage, alors que la phase suggère des propagations vers l'ouest. Aux fréquences plus élevées, l'importance de τ^y est réduite. La description de la PF par un modèle statistique n'incluant que le forçage local, peut mener à une interprétation incorrecte de la dynamique de la PF, particulièrement dans la bande synoptique, où la variance du vent est la plus élevée.

L'énergie originaire d'une source non locale est évidente surtout à $\omega > 0{,}5$ cpj et à des stations de la moitié est du plateau, mais elle joue un rôle important à tous les sites et à toutes les fréquences. Ces variations se propagent vers l'ouest à des vitesses de 6,5 ($\omega < 0{,}2$ cpj), 25–33 ($0{,}2 < \omega < 0{,}5$ cpj), et 12–17m s^{-1} ($\omega > 0{,}5$ cpj). Les échelles de décroissance exponentielle à toutes les fréquences sont d'environ 900 km le long de la direction de propagation de la phase. La réaction non locale est en accord avec les estimations théoriques des premières et secondes harmoniques des ondes de plateau pour cette région, et représente l'évidence la plus directe, obtenue jusqu'à présent, de l'activité des ondes de plateau sur le plateau Scotian.

1 Introduction

Meteorological forcing has been shown to be an important source of energy to Scotian Shelf dynamics at 2–10 d periods (Petrie and Smith, 1977; Smith et al., 1978; Sandstrom, 1980). Because of its intensity, the typical Canadian East Coast winter cyclone can produce sizable fluctuations in sea-level and current. The complete sea-level or current signal is often a complex summation of modes combining energy from local wind forcing and non-locally generated free waves. Spatial irregularities in the wind regime and bottom topography, and the presence of density stratification can further complicate the response. To account for these uncertainties requires simultaneous measurements of sea-level, current, and atmospheric parameters resolved on sufficiently small spatial and temporal scales. CASP provided such an opportunity on the Scotian Shelf. To complement a uniquely concentrated set of meteorological observations, a suite of oceanographic instruments was deployed to measure variations in sea-level, current, water mass properties, and the wave field on two scales: synoptic – O(1000 km) – and mesoscale – O(100 km).

Results from this shelf experiment can be used to address several fundamental questions pertaining to shelf circulation on these scales. The most basic question concerns the nature of the oceanic response to time-dependent meteorological forcing. Although meteorological variations have been shown to be correlated with fluctuations in sea-level and current, the frequency-dependence of this relationship and its dynamical implications are not clearly understood. In addition, the majority of observations previously made on the Scotian Shelf have been restricted to the outer shelf and shelf break regions (Smith et al., 1978; Smith and Petrie, 1982; Petrie, 1983) or have dealt strictly with coastal sea-level (CSL) measurements (Sandstrom, 1980; Thompson, 1986). Because the dynamics of shelf regions near the coast are more sensitive to changes in depth, the concentration of CASP instruments on the inner third of the Scotian Shelf provides new insight into wind-driven motions not readily discernible from coastal or shelf break observations alone.

Another potentially important energy source to the shelf arises from non-local forcing, often seen in the form of coastal trapped waves (CTWs). Petrie and Smith (1977) give indirect evidence for this, but Sandstrom's (1980) results suggest CSL responds as a purely forced wave, driven by the eastward motion of storms. No direct evidence of CTWs has yet been found on the Scotian Shelf. The complete coverage of the CASP bottom pressure and current array provides an excellent and heretofore unavailable source of information for detecting CTWs, if they exist.

The initial analysis of subtidal CASP data concentrates on the response of the subsurface pressure (SSP) field to meteorological forcing. I begin with SSP because it is simple, relatively easy to measure with good precision, and describes the integrated response of the water column. In addition, the SSP signal is a useful diagnostic of local wind forcing as well as CTW modes.

Results are summarized in time series and spectral forms, and a multiple regression analysis is used to describe the frequency-dependent SSP response to local and non-local meteorological forcing. The relative contribution of each component of forcing is discussed as a function of frequency and position on the shelf, and related to simple dynamical theories that may be applicable to the Scotian Shelf.

2 Observations

a *Methods*

The data described and analysed in this paper were obtained during the CASP field experiment. Instruments were deployed on the Scotian Shelf for a period from November 1985 to April 1986 to measure oceanic responses on mesoscale and synoptic meteorological forcing scales (Fig. 1).

An array of bottom pressure gauges deployed along the length of the Nova Scotia coast, supplemented by Canadian Hydrographic Service permanent tide-gauges, monitored synoptic-scale variations of order 1000 km. From west to east, the temporary gauges were located at West Head, Riverport, Sambro, Ship Harbour, Whitehead Harbour and Louisbourg. Permanent sites included Yarmouth, Halifax, North Sydney and Port aux Basques, Newfoundland.

An offshore mooring array consisted of two cross-shelf lines near Halifax (S1–S5) and Liscomb (S9–S11), and a series of moorings along the 100-m isobath (S2, S6–S8, S10). The array was designed to detect mesoscale variations in the current and pressure fields on scales of order 100 km. Bottom-mounted pressure gauges were deployed at stations S1–S10. Pressure gauges were Aanderaa WLR-5 Water Level Recorders with a range of 0–400 psi* and an accuracy of 0.04 psi. With the exception of S3, data return was of high quality.

Tide-gauge data were isostatically adjusted with local atmospheric pressure at each site to be compatible with bottom pressure records. All bottom pressure and adjusted sea-level will be referred to as subsurface pressure (SSP) throughout this paper. The series were low-pass filtered with a 129-weight Cartwright filter (0.036 cph (28 h) half-power cut-off) to remove tidal and inertial energy and were resampled at six-hourly intervals.

Wind (τ) and atmospheric pressure (p^a) data from the Sable Island AES station

*1 psi ≡ 6.89 kPa.

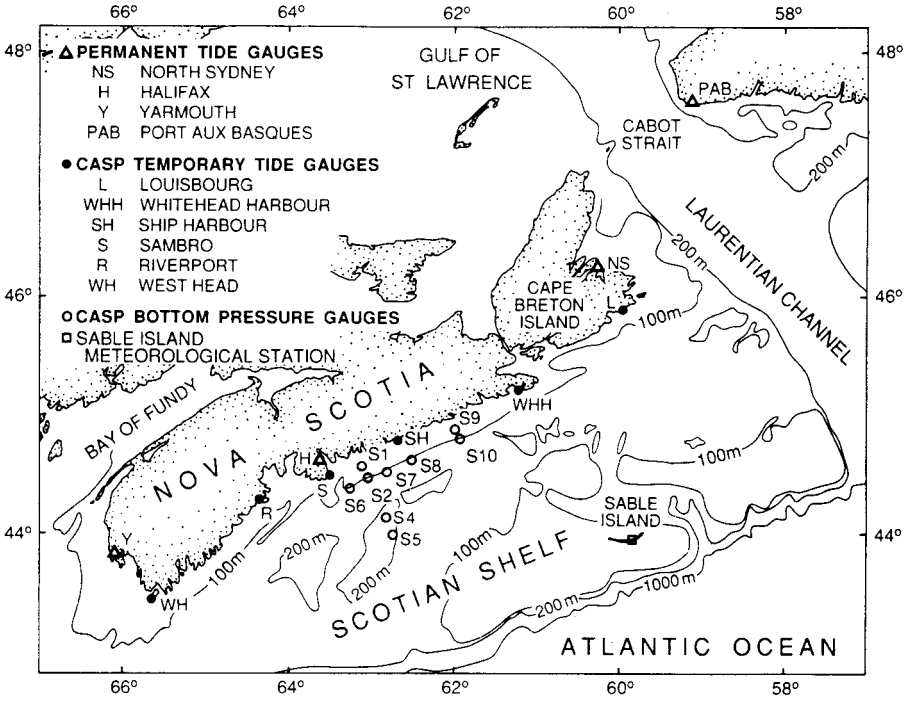

Fig. 1 Map showing positions of bottom pressure (circles) and permanent tide-gauge (triangles) stations, and the meteorological station at Sable Island (square).

(Fig. 1) were chosen to represent meteorological conditions over the Scotian Shelf (Petrie and Smith, 1977). Alongshelf ($+\tau^y = 68°$T) and cross-shelf ($+\tau^x = 158°$T) wind stress components were estimated from wind speed and direction, using the quadratic stress law with a variable drag coefficient (Smith and Banke, 1975). The wind stress and pressure series were filtered and resampled in the same manner as the SSP series. Additional information on the processing of CASP data is given by Lively (1987).

Autospectral variance for all series was calculated according to Carter and Ferrie (1979). The 32 frequency bands each had a bandwidth of 0.0625 cpd. Spectral results were averaged over $n = 14$ blocks of data with 50% overlap, giving $\nu = 22.9$ effective degrees of freedom (Garrett and Toulany, 1982).

b *Time Series*

Low-passed time series plots comparing SSP at stations along the coast and the Halifax line exhibit a high degree of correlation over the entire pressure field (Fig. 2). SSP is also visually quite coherent with alongshelf wind stress. Stress to the east (west) generated a set-down (set-up) of sea-level over the entire shelf, consistent with a cross-shelf surface Ekman flux. These wind-driven events, which occurred in association with the passage of winter atmospheric cyclones, were periodic at about

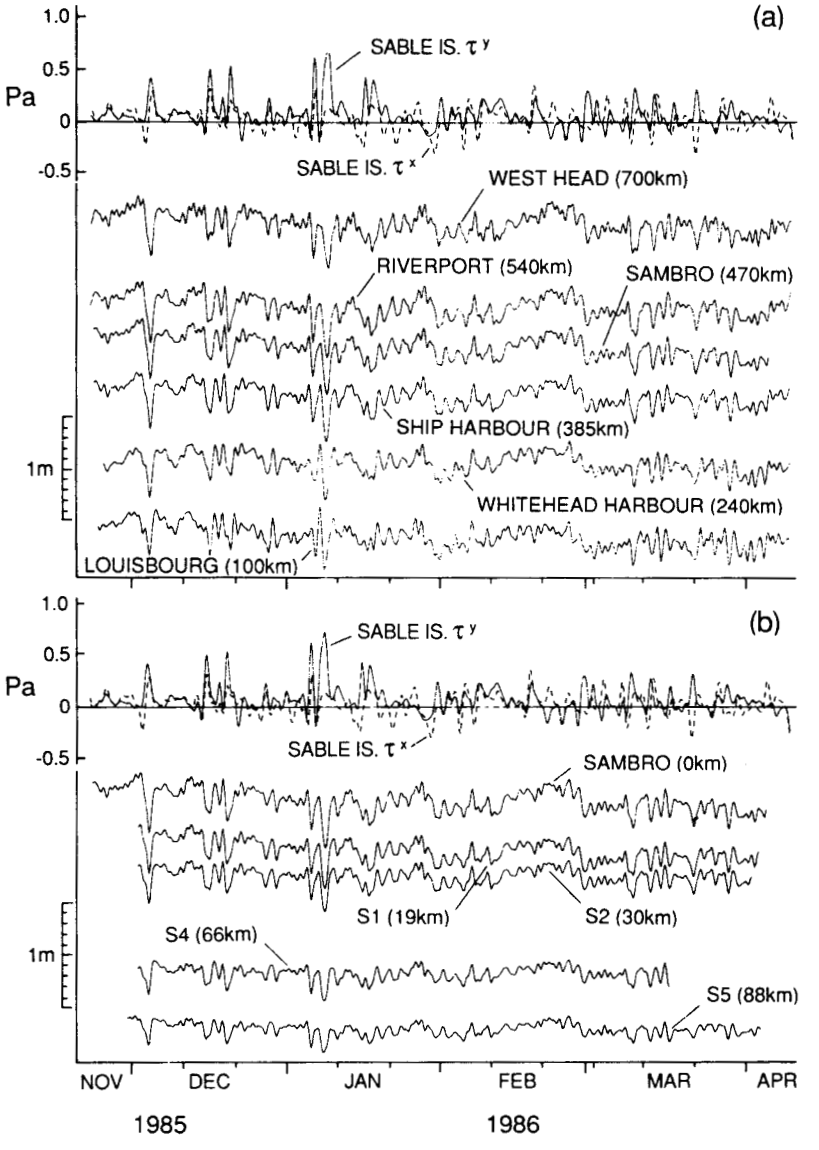

Fig. 2. Time series of Sable Island cross-shelf (τ^x) and alongshelf (τ^y) wind stress components, and bottom pressure from (a) coastal and (b) Halifax line (S1–S5) gauges. Series have been low-pass filtered and resampled at 6-h intervals. Distance relative to the (a) Laurentian Channel or (b) coast as shown.

2 d with an amplitude of 15–30 cm at the coast. However, the response can be much larger, as evidenced by a 60-cm coastal set-down during a one-Pa easterly stress on 7 January. A very low frequency trend is also discernible throughout the records.

Although not apparent at the scale shown, an east-to-west phase propagation was detected in coastal SSP as well, opposite that of the typical storm track. A similar

pattern appeared in the 100-m isobath series. No consistent change in amplitude was evident in the coastal SSP records, although the standard deviations of the series, which vary from 9 to 12 cm, generally increased to the west.

SSP also displayed a large cross-shelf coherence scale. The amplitude of SSP decreased by a factor of about two from the coast to S5, approximately 90 km offshore. Note that the cross-shelf slope (i.e. the difference between S1 and S5) decreased over time, presumably owing to a decreased outflow from the Gulf of St Lawrence (Drinkwater et al., 1979). A slight onshore phase propagation is seen in the Halifax line, although it is approximately an order of magnitude smaller than that of the alongshelf direction.

c *Autospectral Variance*

Both Sable Island wind stress components exhibited a similar frequency distribution of variance, as shown by their spectra plotted in variance-preserving form (Fig. 3a). A majority of variance (50–65%) was concentrated in the 0.2–0.5 cpd band, although a significant amount (20–30%) occurred at lower frequencies ($\omega \leq 0.125$ cpd). The alongshelf stress component (τ^y) was more energetic at all frequencies except 0.313 cpd. Sable Island atmospheric pressure (p^a) showed a similar variance distribution, although this autospectrum contained relatively less energy at $\omega > 0.3$ cpd.

SSP spectra generally reflected a variance distribution similar to the meteorological signals. As expected from the visually correlated time series (Fig. 2), the spectra exhibited a similar distribution of variance at most coastal locations (Fig. 3b). Approximately 50% of the subtidal variance occurred in the 0.2–0.5 cpd band, with a large decrease in variance at $\omega > 0.438$ cpd coinciding with the τ^y spectrum. Again considerable energy ($\sim$ 40%) was contained at $\omega \leq 0.125$ cpd.

Coastal SSP generally increased in variance from east to west, most notably at $\omega <$ 0.5 cpd. An exception to this occurred at stations adjacent to the Cabot Strait, where SSP variance at 0.563 cpd was noticeably greater at North Sydney (not shown) and Louisbourg (Fig. 3b). This signal was even stronger at Port aux Basques, on the Newfoundland side of the Strait. It also appears that energy at this frequency does not propagate effectively as shown on the spectral distribution at Whitehead Harbour, only 140 km west of Louisbourg.

SSP variance decreased uniformly with distance offshore in all frequency bands (Fig. 3c). The variance dropped by a factor of two to three over a distance of $\sim$ 100 km, consistent with the time series. The importance of the 0.2–0.5 cpd band was again seen at all locations, but the relative contribution at the lowest frequencies was reduced at the offshore stations (30 vs 40%). Overall, however, the SSP spectra, like the time series, were similar over the entire Scotian Shelf region in the along- and cross-shelf directions. The close agreement with the distribution of variance in the meteorological spectra suggests that local meteorological forcing is an important source for subtidal SSP oscillations.

3 Dynamical model

The total SSP signal at any location on the Scotian Shelf can be expressed as

$$\eta(x, y, t) = \eta^L(x, y, t) + \eta^{NL}(x, y, t). \tag{3.1}$$

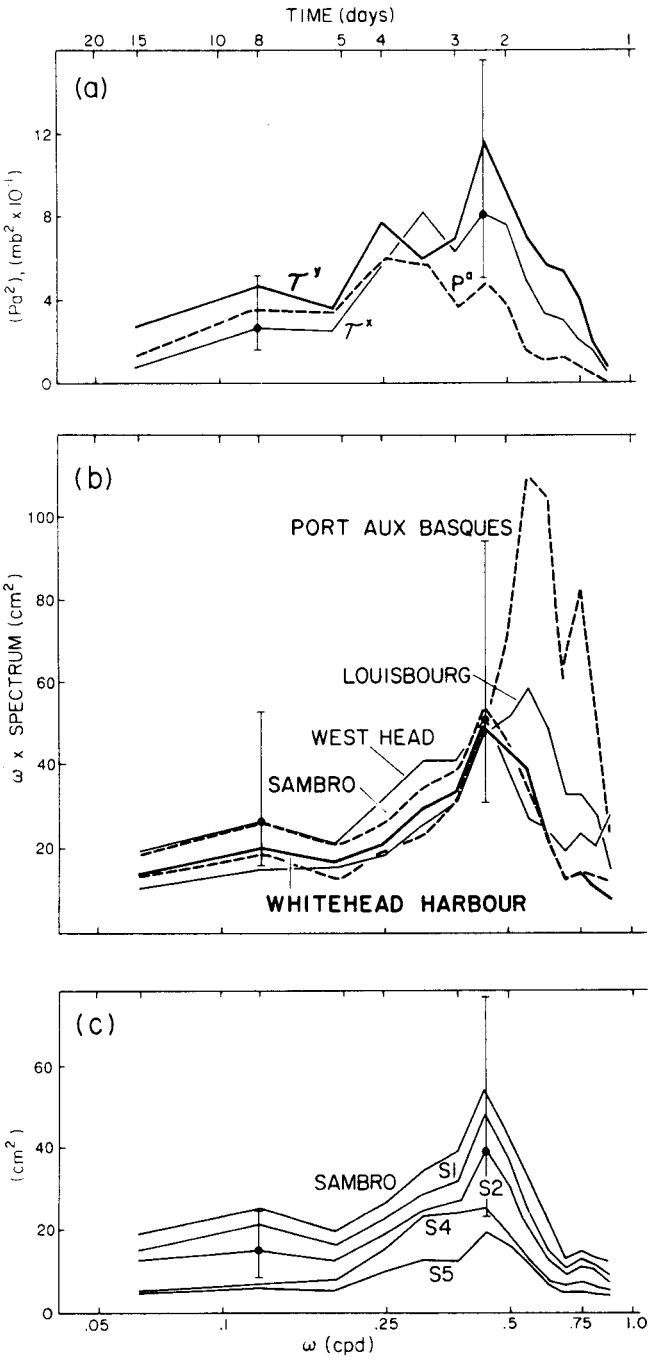

Fig. 3 Autospectra (variance preserved) of low-pass filtered time series for (a) Sable Island wind stress and atmospheric pressure, (b) coastal bottom pressure and (c) bottom pressure from the Halifax line. Representative 95% confidence intervals are shown.

The term η^L defines the locally-forced influence, i.e. the response of SSP to wind stress over the Scotian Shelf. That portion of η whose origin lies beyond the Scotian Shelf is defined by η^{NL}, the free contribution to SSP. These two terms are not necessarily statistically independent, since non-locally forced (free) waves may be generated by a wind stress coherent with that over the Scotian Shelf. These two effects can, however, be separated through a combination of statistical and dynamical arguments.

Initially consider η^L, the expected response of SSP to local wind stress, based on a dynamical shelf model. Assume a long, straight coastline with a right-handed coordinate system such that $x = 0$ at the coast and increases in the offshore direction. Forcing is by a time-varying alongshelf kinematic wind stress $\tau = \tau_0 e^{i\omega t}$. The dynamical model is based on the following homogeneous, linearized, shallow water momentum and continuity equations:

$$-fv = -g\eta_x \tag{3.2}$$

$$v_t + fu = -g\eta_y + \frac{\tau}{h} - \frac{rv}{h} \tag{3.3}$$

$$(uh)_x + (vh)_y = 0 \tag{3.4}$$

where u and v are depth-averaged current velocities in the x (cross-shelf) and y (alongshelf) directions, respectively; η is the local, wind-forced contribution to sea surface elevation (η^L in (3.1)); f is the (constant) Coriolis acceleration; g is the acceleration due to gravity; and r is the linear bottom friction coefficient. Subscripts denote partial differentiation. Harmonic time-dependence of the form $e^{i\omega t}$ is assumed for all time derivatives.

Equation (3.2) has been simplified to a geostrophic balance by taking $\omega/f \ll 1$ and assuming the long-wave approximation $\ell L \ll 1$, where ℓ is the horizontal length scale of the forcing and L is the shelf width. The rigid lid approximation ($\eta_t = 0$) is also made in (3.4). Substituting (3.2) and (3.3) into (3.4) provides a governing equation expressed solely in terms of η;

$$\left(\epsilon h\eta_x - \frac{\tau}{g}\right)_x + h_x\eta_y - h_y\eta_x = 0, \tag{3.5}$$

where

$$\epsilon = \left(i\frac{\omega}{f} + \frac{r}{hf}\right)$$

Eqn. (3.5) is identical to the equation Wright (1986) used to examine the quasi-steady limits of coastal-trapped circulation.

For simplicity, assume an idealized topography that is uniform alongshelf; i.e. $h = h(x)$, and a spatially uniform wind stress; i.e. $\tau = \tau(t)$, at least over a scale ℓ^{-1} much greater than L. These assumptions reduce (3.5) to

$$(\epsilon h\eta_x)_x + h_x\eta_y = 0, \tag{3.6}$$

a parabolic partial differential equation analogous to the heat diffusion equation with

$y < 0$ (i.e. downshelf, in the direction of propagation for free CTWs) replacing the time axis. Thus a disturbance at some point in the field diffuses in the x-direction for increasingly negative y. The steady-state limit of (3.6) is the arrested topographic wave (Csanady, 1978). Other limits and applications of (3.6) are detailed in Wright (1986).

To apply (3.6) to the Scotian Shelf, the bottom topography is treated as a simple-wedge-step shelf profile;

$$h\begin{cases} = h_1\left(\dfrac{x}{L_1}\right) & 0 < x < L_1 \\ = h_1 & L_1 < x < L \\ = \infty & x > L \end{cases} \tag{3.7}$$

For the Scotian Shelf the wedge and step regions are approximately equal in width ($L \approx 2L_1$). The CASP mooring array was concentrated in the region $0 < x < L_1$, where the most dynamically interesting responses should take place. Within the wedge region $h = sx$, where s is the slope ($= h_1/L_1$), and (3.5) can be expressed as

$$(\epsilon x \eta_x)_x + \eta_y = 0 \qquad 0 < x < L_1. \tag{3.8}$$

In the step region of the shelf $s = 0$, and the solution of (3.6) is trivial.

The boundary conditions are

$$\eta_x(y) = \frac{\tau f}{gr} \qquad x = 0 \tag{3.9}$$

$$\eta(y) = 0 \qquad x = L \tag{3.10}$$

$$\eta_x(y) = \frac{\eta}{L_1 - L} \qquad x = L_1 \tag{3.11}$$

$$\eta(x) = 0 \qquad y = 0. \tag{3.12}$$

Equation (3.9) is obtained because the constraint of no mass flux through the coast requires $v(0, y) = \tau/r$, a balance between surface stress and bottom friction, as $h \to 0$ (from (3.3)). To keep the geostrophic transport across the shelf break finite requires $\eta_y = 0$ at $x = L$. Since $\eta = 0$ at $y = 0$, it follows that (3.10) must be valid. Because $\epsilon h \eta_{xx} = 0$ for $L_1 < x < L$, η is a linear function of x over the uniform depth region. Since η *and* η_x must be continuous over the change in topography at $x = L_1$ (so that uh is continuous), (3.11) is obtained by evaluating η just inshore of L_1 and differentiating.

Equation (3.12), hence (3.10), presumes η set to zero at some cross-shelf boundary $y = 0$. For the Scotian Shelf, we prescribe $\eta = 0$ at Louisbourg, near the Laurentian Channel (Fig. 1), an appropriate condition if little wind-forced variation in SSP traverses this deep channel. This is a critical boundary condition, since it assumes the Louisbourg SSP signal is associated solely with motions generated remote from the Scotian Shelf. Thus non-locally generated CTWs will be excluded from the solution to (3.6). As Wright et al. (1986) have previously pointed out, the steady response is

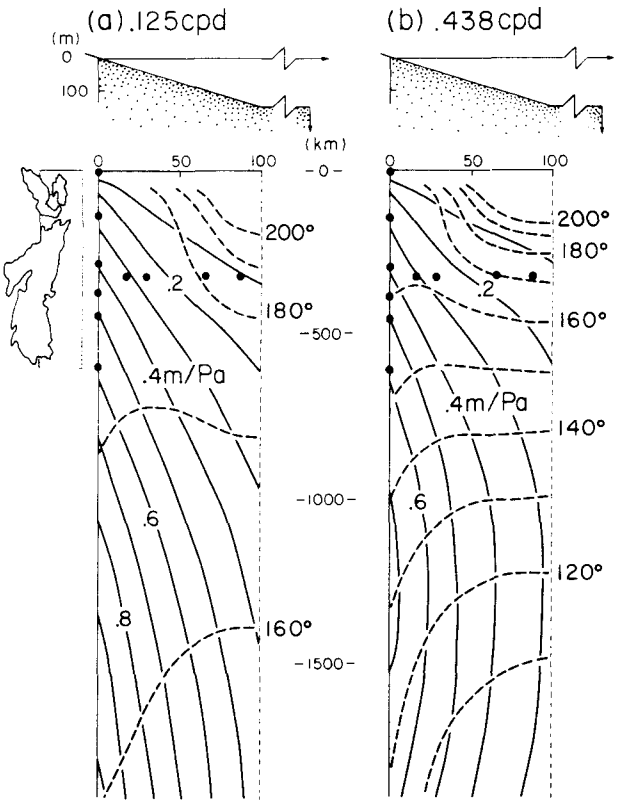

Fig. 4 Solution to Eq. (3.5) for (a) 0.125 cpd and (b) 0.438 cpd for $r = 10^{-3}$ m s^{-1}, $L_1 = 100$ km, $L = 200$ km and $h_1 = 150$ m, and the offshore topography shown. Solid lines define the amplitude (m Pa^{-1}); broken lines define the phase by which η leads τ. Approximate positions of the pressure gauges within the model domain are noted.

highly sensitive to changes in the cross-shelf condition. Thus solutions to (3.6) subject to (3.12) represent only that portion of SSP forced by *local* wind stress (i.e. directly over the model domain), and may be unsatisfactory in describing the *entire* SSP signal on the Scotian Shelf, depending on the magnitude of η^{NL} in (3.1). For simplicity any variation in SSP attributed to wind stress over the shelf region will be defined as the "local" response, while the signal at Louisbourg will be defined as the "non-local" contribution. An alternative to (3.12) could be $\eta = \eta^0$, where η^0 describes the form of the SSP signal observed at $y = 0$; (e.g. a series of CTW modes).

The amplitude and phase of η over the wedge region of the shelf are presented for two different frequencies of alongshelf wind stress forcing; 0.125 cpd (Fig. 4a) and 0.438 cpd (Fig. 4b). These results were obtained by solving (3.6) numerically using boundary conditions (3.9–3.12), and assuming typical values of $r = 10^{-3}$ m s^{-1}, $L_1 = 100$ km, $L = 200$ km and $h_1 = 150$ m. The distance between Louisbourg and West Head is about $3L$. Amplitude is expressed in units of m Pa^{-1}. Positive phase indicates η leads τ. The approximate positions of the SSP sites whose time series are presented in Fig. 2 are marked for reference.

Several important circulation features are apparent in Fig. 4. The amplitude of the response increases in the direction of free wave propagation and decreases offshore, similar to the steady response found by Csanady (1978). Phase decreases to the west, indicating a propagation of sea-level in the direction consistent with free waves. Friction becomes less dominant at higher frequencies, and alongshelf phase speed increases while the cross-shelf slope decreases. At some distance downshelf, terms that vary in y become small and the cross-shelf mass flux $uh \rightarrow 0$, from (3.4) and the requirement $u = 0$ at the coast. Alongshelf velocity becomes steady, proportional to τ, and decreases with increasing ω. From (3.2) and (3.3) sea-level at any position sufficiently far downshelf is

$$\eta(x) = \frac{\tau f}{gr} \int_x^L \left(1 + \frac{i\omega h}{r}\right)^{-1} dx \tag{3.13}$$

a constant along any isobath. Physically the amplitude is limited by temporal variations in the forcing and the subsequent phase interference of free waves generated at different locations along the shelf.

4 Statistical models

To describe the response of the SSP field to wind stress forcing, a hierarchy of multiple linear regression models in the frequency domain was implemented (Jenkins and Watts, 1968; p. 493). The three models compared here are

$$S(\omega) = \alpha_1 T^y(\omega) + \beta_1 T^x(\omega) + \epsilon_1(\omega) \tag{4.1}$$

$$S(\omega) = \alpha_2 T^y(\omega) + \beta_2 T^x(\omega) + \gamma_2 S^{NL}(\omega) + \epsilon_2(\omega) \tag{4.2}$$

$$S(\omega) = \gamma_3 S^{NL}(\omega) + \epsilon_3(\omega). \tag{4.3}$$

The variables S, T^y, T^x and S^{NL} in (4.1–4.3) define Fourier transforms of the variables SSP, τ^y, τ^x and SSP^{NL}, respectively, where SSP^{NL} (approximated by Louisbourg SSP) is a representation of the non-locally forced contribution to SSP. The coefficients α_i, β_i and γ_i are complex transfer functions and ϵ_i is the residual error associated with each model. Least-squares estimates of α_i, β_i and γ_i give the amplitude and phase of the SSP response to each individual forcing term as well as the multiple coherence squared (R_i^2) due to the model for each frequency band. Garrett and Toulany (1982) provide further details of this technique. A comparison can be drawn between this method and that applied by Freeland et al. (1986) in the time domain.

To aid in the interpretation of the statistical analyses, results are described for specific key frequencies representing three bands of interest in the low-passed spectra. Variability at frequencies below the dominant wind band ($\omega < 0.2$ cpd) is represented by 0.125 cpd. The peak of maximum variance in the majority of SSP spectra (0.438 cpd) represents fluctuations in the synoptic band (0.2–0.5 cpd). Results at 0.625 cpd describe the response in the band between maximum wind and tidal forcing (0.5–1.0 cpd). The models (4.1–4.3) will be referred to as models L, L + NL, and NL, respectively, where L implies local and NL non-local forcing effects are included.

a *Local Forcing*

Recall that the "local" forced response refers to that portion of SSP due to a (presumed) homogeneous wind stress over the Scotian Shelf, represented by Sable Island stress. Although wind forcing near the eastern boundary of the shelf undoubtedly generates motions that propagate freely to the west, such motions are considered part of the locally forced response in the statistical models.

With a few minor exceptions, the alongshelf wind stress component τ^y was the dominant wind-forcing term in models L and L + NL (4.1–4.2), with the cross-shelf component τ^x of only secondary importance. Atmospheric pressure p^a was generally an unimportant contributor to SSP when added to L. Further, the SSP response to p^a and, to a lesser extent, τ^x was not statistically significant once τ^y effects were considered. It is therefore believed that τ^y is the principal source of energy to the SSP field via local meteorological forcing, in agreement with the forcing prescribed in the dynamical model of Section 3. Description of the statistical models transfer functions will be limited to τ^y. Results from models L and L + NL are summarized in Figs 5–7 in terms of the amplitude and phase of the SSP response at the coastal stations and S1–S5, the cross-shelf line.

The response to τ^y allows Scotian Shelf SSP observations to be related to the time-dependent solution given by the wind-forced dynamical model in the previous section. The transfer function at 0.125 cpd in both statistical models (Fig. 5) featured a pattern similar to that of the dynamical model. From east to west, the modulus or amplitude $|\alpha_i|$ of the gain increased while the phase ϕ_i decreased slightly, opposite that of a typical low-pressure system that deepens and intensifies as it moves eastward through the region. Both ϕ_i and $|\alpha_i|$ decreased in the offshore direction. The addition of p^a into model L had no effect on SSP response to τ^y, but the additional term SSP^{NL} in L + NL acted to substantially reduce $|\alpha_2|$ and bring ϕ_2 closer to 180° at all sites, relative to $|\alpha_1|$ and ϕ_1. For a 1-Pa alongshelf wind stress to the west, sea-level at the coast rose by 30–70 cm (e.g. 62 cm at Sambro) according to model L, but only 0–50 cm (42 cm at Sambro) by L + NL.

At 0.438 cpd an even greater difference in statistical model results was seen (Fig. 6). $|\alpha_1|$ was larger relative to lower frequencies, but little systematic change in $|\alpha_1|$ was apparent along the coast. In contrast, $|\alpha_2|$ exhibited a pattern similar to that seen at 0.125 cpd. In particular note how $|\alpha_2|$ extrapolates to zero near the Cabot Strait, while $|\alpha_1|$ values are much greater at the upshelf boundary. This is apparent at higher frequencies as well. The difference between $|\alpha_1|$ and $|\alpha_2|$ at 0.438 cpd was also greater than that at 0.125 cpd at all sites. Alongshelf ϕ_1 and ϕ_2 variations imply a similar westward motion. At all sites ϕ_i was farther from 180° than observed at lower frequencies, presumably owing to the decreased importance of friction as seen in the dynamical model.

The SSP response to τ^y at 0.125 and 0.438 cpd as determined from models L and L + NL are also compared with the dynamical model solutions in Figs. 5 and 6. This relatively simple model, with idealized topography and alongshelf homogeneity, does a reasonable job of estimating the amplitude of the wind-forced response and describing the patterns of this response for the Scotian Shelf.

Finally, consider the response to τ^y at frequencies higher than those of the synoptic band; e.g. 0.625 cpd (Fig. 7). The alongshelf and cross-shelf pattern of $|\alpha_i|$ was

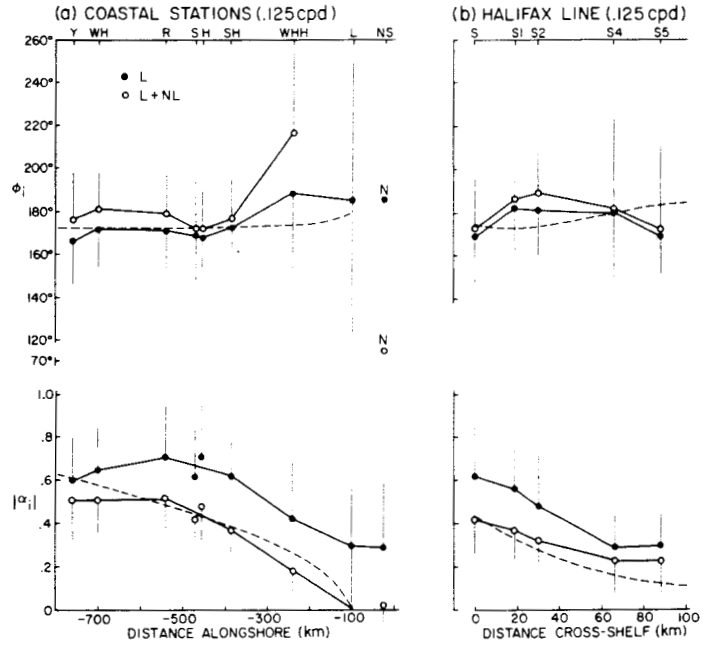

Fig. 5 Phase ϕ_i and amplitude $|\alpha_i|$ of SSP response to Sable Island alongshelf wind stress τ^y at 0.125 cpd for (a) coastal stations and (b) the Halifax line. Solid circles represent the response from model L, open circles represent the response from model L + NL. Errors bars represent the 95% confidence limits. The absence of error bars denote sites where $|\alpha_i|$ is not significantly different from zero. SSP leads τ^y by ϕ_i. Broken lines denote dynamical model results, taken from Fig. 4.

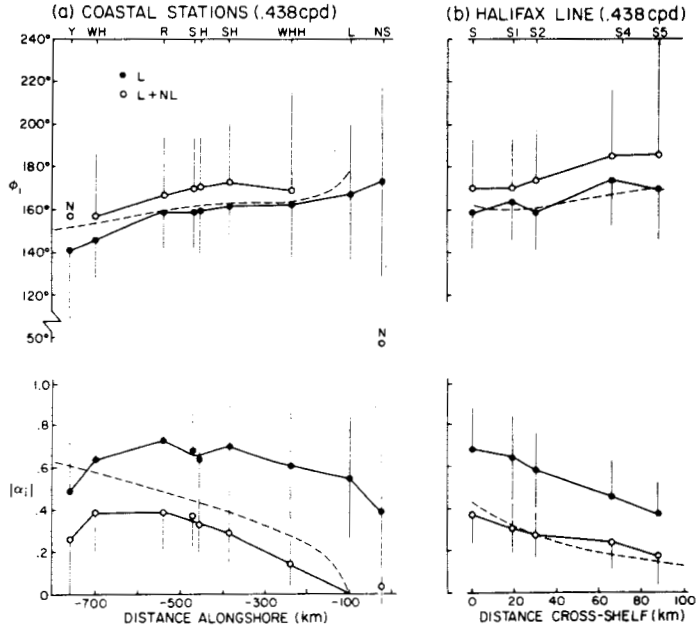

Fig. 6 As for Fig. 5, except for 0.438 cpd.

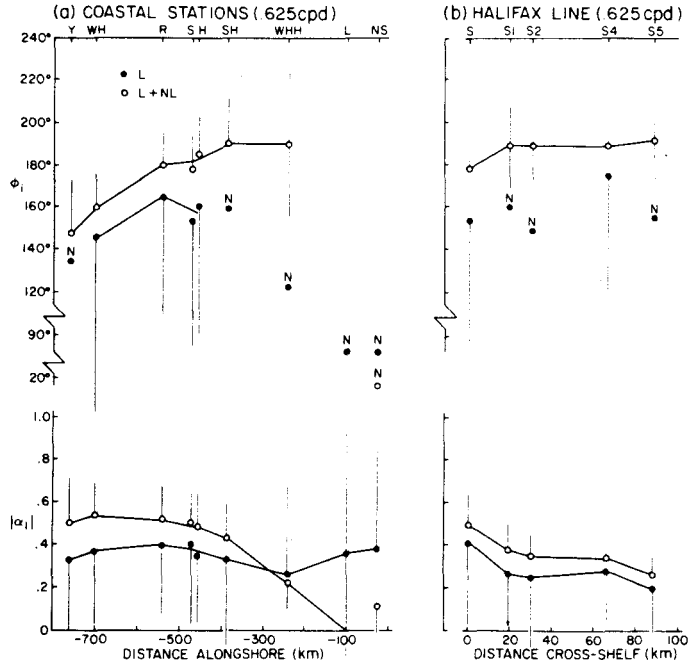

Fig. 7 As for Fig. 5, except for 0.625 cpd.

similar to that seen at 0.438 cpd, although values of $|\alpha_1|$ were much smaller, and of $|\alpha_2|$ larger at the higher frequency. The difference between ϕ_1 and ϕ_2 was also larger; ϕ_2 showed a consistent decrease of $\sim 40°$ along the coast from Whitehead Harbour to Yarmouth, whereas the direction of propagation implied by ϕ_1 was somewhat ambiguous. The cross-shelf ϕ_i exhibited no directional preference.

In summary, alongshelf wind forcing is an important source of energy for SSP oscillations over the inner Scotian Shelf. However, the inclusion of non-local influences in the statistical model substantially reduces the estimated response of SSP attributed to local τ^y alone. This is particularly true in the synoptic band, where $|\alpha_2|$ replicates the pattern of the dynamical model while $|\alpha_1|$ has large amplitudes and no alongshelf trend. The disparity between models L and L + NL demonstrates that statistical results may lead to improper conclusions if not reinforced by some physically relevant theory. Thus it is essential to include non-local forcing to obtain a reasonable representation of the subsurface pressure field.

b *Non–local Forcing*

The additional term in model L + NL contains the complex transfer function γ_2, which accounts for SSP variations after local forcing effects due to wind stress have been removed. Therefore any free wave energy propagating onto the shelf will be accounted for by the non-local forcing term. Louisbourg SSP is defined as the non-locally forced contribution to SSP. Results consistent with the dynamical model indicate the response to Sable Island wind stress at Louisbourg was small at low

frequencies, suggesting the SSP signal there contained a significant amount of energy originating from a distant source. The anomalous autospectrum at Louisbourg also indicated this was true at higher frequencies as well. Finally, its location adjacent to the Cabot Strait makes Louisbourg SSP a good diagnostic of energy crossing the Laurentian Channel or propagating out of the Gulf of St Lawrence.

The response to SSP^{NL} in L + NL featured a similar pattern at all frequencies, although the magnitude and degree of change were somewhat frequency-dependent (Figs 8–10). In general, $|\gamma_2|$ decreased to the west and offshore, and the phase direction was to the west. At the lowest frequencies (Fig. 8) $|\gamma_2|$ decreased by factors of two and three over the alongshelf (600 km) and cross-shelf (100 km) length scales of the arrays, respectively. Phase ϕ_2 decreased smoothly along the coast, but the cross-shelf change was less certain. Alongshelf $|\gamma_2|$ changed similarly at 0.438 cpd, but the cross-shelf decrease was markedly reduced (Fig. 9). Alongshelf ϕ_2 was again consistent with free-wave propagation. The general pattern was most obvious at 0.625 cpd (Fig. 10).

As noted above, the transfer functions between SSP and τ^y were sensitive to whether or not the SSP^{NL} term was included in the model. The response to SSP^{NL} also changed with the inclusion of wind forcing in the regression. Model NL defines the correlation between SSP at Louisbourg and other sites. Estimates of SSP coherence scales at each frequency may be made from these results.

It is important to note the substantially different exponential decay scales of SSP, depending upon whether or not local forcing is removed. In contrast with the results from L + NL, $|\gamma_3|$ no decrease from unity away from Louisbourg at 0.125 and 0.438 cpd, but increased alongshelf to values of 1.1–1.2 (Figs 8 and 9). The increase in spectral variance along the coast at $\omega < 0.5$ cpd (Fig. 3) is reflected in this result, implying a coherence scale at least 600 km. At 0.625 cpd, however, $|\gamma_3|$ decreased precipitously downshelf of Louisbourg, suggesting an exponential decay scale of ~300 km (Fig. 10). Again this is consistent with the pattern in the spectral variance. The distribution of ϕ_3 along the coast at all frequencies indicates a westward propagating SSP signal, similar to ϕ_2.

At all frequencies $|\gamma_2|$ and ϕ_2 exhibit an excellent fit as a function of distance y downshelf from Louisbourg. Best fits of the form $\hat{\phi}_2 = a + by$ and $|\hat{\gamma}_2| = ce^{dy}$ were made for each set of values from the coastal stations. The North Sydney response is included for reference.

From b, the slope of the ϕ_2 linear regressions, a phase speed can be determined. Phase speed was westward at all frequencies, consistent with the expected free-wave propagation. The magnitude of the slope varied with frequency. Knowing the slope and associated standard error a phase speed, $c = \omega/b$, was estimated with an appropriate standard error for each frequency.

At 0.125 cpd, $c \approx 6.5$ m s^{-1} with the standard error giving a range of 5–10 m s^{-1}. The phase speed at 0.438 cpd was $c \approx 26$ m s^{-1} (S.E. = 22–33 m s^{-1}), while $c \approx 16$ m s^{-1} (S.E. = 13–20 m s^{-1}) at 0.625 cpd. A dispersion diagram was constructed (Fig. 11), with $k = b/2\pi$, by similarly estimating the phase speed at each frequency band. For comparison, phase-speed estimates for the Kelvin wave ($c = (gH)^{1/2}$), shelf wave for a step shelf ($c = fL$), and first and second mode shelf waves for a wedge shelf ($c_1 = 0.7fL$, $c_2 = 0.13fL$) have been added to the figure. These approximations are based

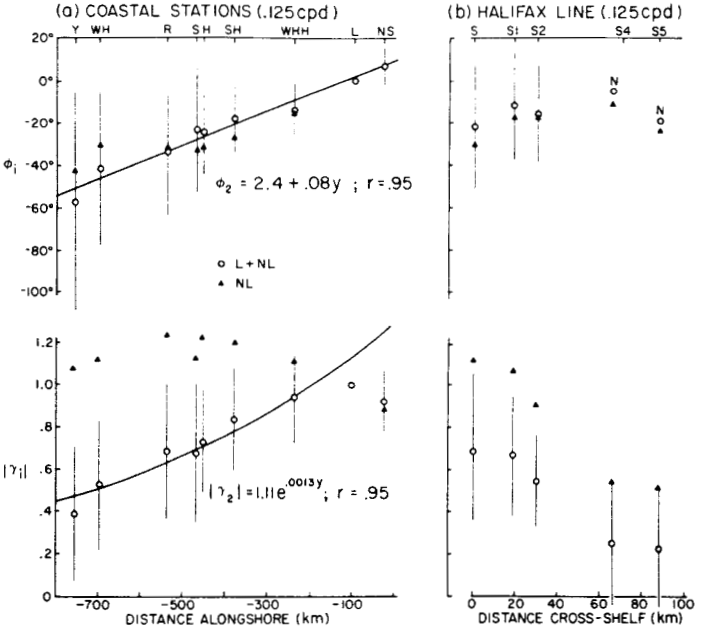

Fig. 8 Phase ϕ_i and amplitude $|\gamma_i|$ of SSP response to SSP^{NL} at 0.125 cpd for (a) coastal stations and (b) the Halifax line. Circles represent the response from model L + NL, and triangles represent the response from model NL. Error bars (95% confidence intervals) are included only for ϕ_2 and $|\gamma_2|$. Bold lines denote the best linear and exponential regression fits to ϕ_2 and $|\gamma_2|$, respectively, as a function of distance y downstream from Louisbourg.

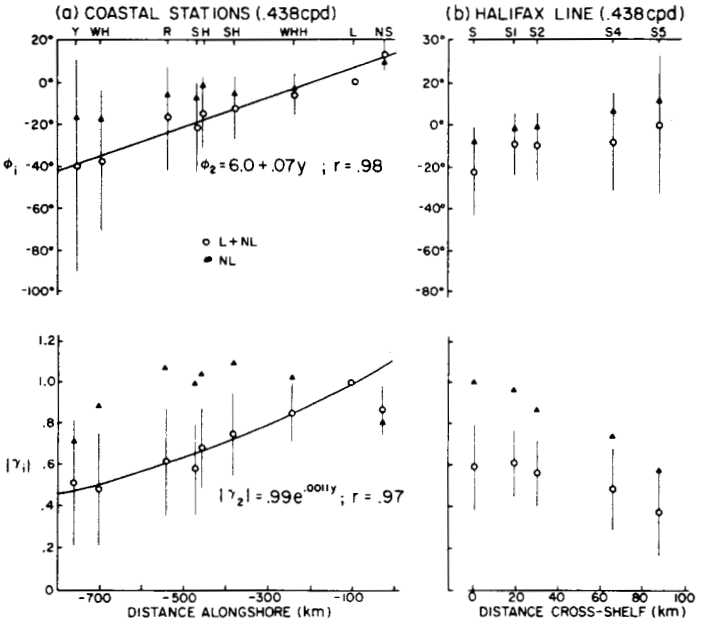

Fig. 9 As for Figure 8, except for 0.438 cpd.

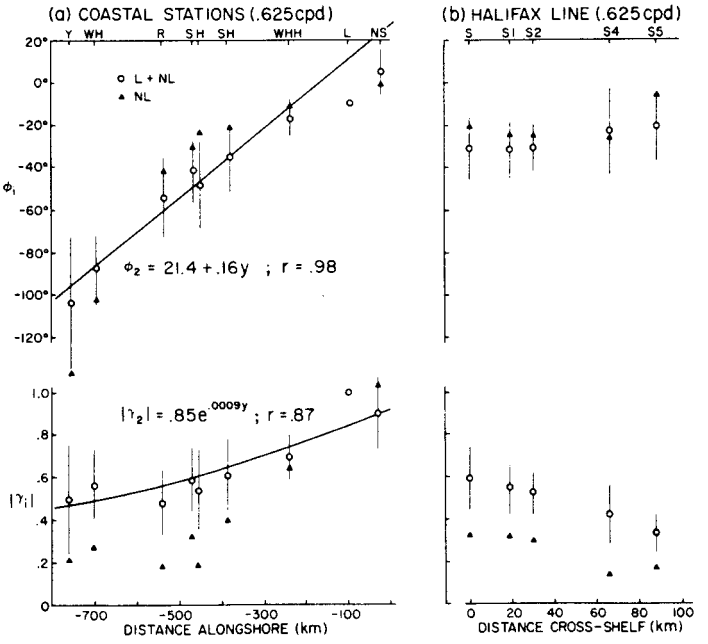

Fig. 10 As for Fig. 8, except for 0.625 cpd.

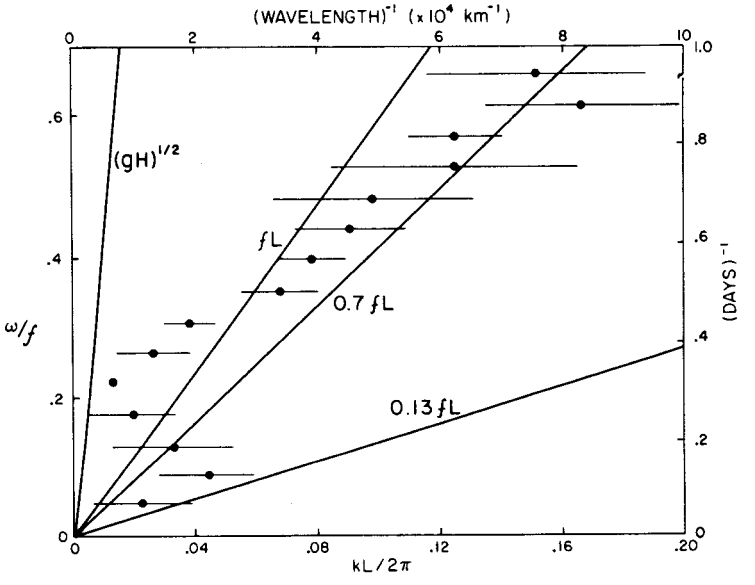

Fig. 11 Dispersion diagram comparing free-wave phase speed for each frequency band with phase speeds for Kelvin wave, step-shelf shelf wave ($c = fL$), and first ($0.7fL$) and second ($0.13fL$) mode wedge-shelf shelf waves (H = 2000 m, L = 200 km, $f = 10^{-4}$ s^{-1}). The circles represent phase speeds (± standard error) determined from the regression of phase on alongshore distance at each frequency, as shown in Figs 8a–10a.

on coastal trapped wave (CTW) theory from Huthnance (1981) using a deep water depth $H = 2000$ m and shelf width $L = 200$ km.

The three frequency bands examined previously separate themselves according to phase speed. For $\omega > 0.5$ cpd, phase speeds were 12–17 m s^{-1}, falling neatly between the lowest mode shelf wave speeds for the two extremes in shelf profile. However, the propagation was not necessarily uniform along the length of the coast. The phase speed at 0.625 cpd decreased to the west, corresponding to a narrowing shelf. From Louisbourg to Riverport ($\sim$ 400 km) the phase lag was $\sim 40°$, giving $c \approx 26$ m s^{-1}. From Riverport to West Head a similar lag occurred over only 200 km, thus $c \approx 13$ m s^{-1}. Estimating the shelf width as narrowing from 250 to 150 km yields a decrease in free wave speed ($c = fL$) from 25 to 15 m s^{-1}, in close agreement with the observed change in speed. Thus not only do shelf waves appear to propagate along the Scotian Shelf, but phase speeds suggest the waves slow down along the narrowing shelf.

Phase speeds at $\omega < 0.2$ cpd were $\sim$ 6.5 m s^{-1}, about twice the second mode speed. Those in the 0.2–0.5 cpd band were 25–33 m s^{-1}, twice those observed at higher frequencies and greater than the maximum possible lowest CTW mode phase speed. Thus although the high-frequency phase speed was directly interpretable as a single mode wave, propagations at lower frequencies suggested a more complex model structure. These discrepancies are not too surprising, since numerous other studies of CTW motions have found that the observed phase speeds can be as much as 2–4 times greater than those predicted by theory (cf. Schwing et al., 1988). The non-local portion of the response found by Freeland et al. (1986), determined with a method very similar to the multiple regression technique applied here, also demonstrated that free motions propagate at speeds about 25% greater than theory would suggest.

The amplitude of the SSP response to non-local forcing also decreased uniformly to the west with an exponential decay scale of ~900 km at all frequencies. The alongshelf decay scales of first and second mode frictional shelf waves should be approximately 1200 and 200 km, respectively, for the appropriate Scotian Shelf parameters. The lowest mode estimate agrees reasonably with the observations, although the scale for the second mode is smaller than those seen. A more detailed analysis is required to determine the modal structure of the free response. However, the character of the non-local response strongly suggests that CTW activity is important, and is the most direct evidence of shelf waves on the Scotian Shelf to date.

c *Comparison of Local and Non-local Forcing*

Figure 12 summarizes the multiple coherence squared (R^2) attributed to the three statistical models. The triangles represent the amount of variance in each coastal SSP signal explained by model NL. R_3^2 decreased away from Louisbourg at all frequencies. A comparison of R_3^2 values at 0.125 and 0.438 cpd (Figs 12a and b) with those at 0.625 cpd (Fig. 12c), which drop to zero only 300 km downshelf, suggests that SSP coherence length scales were smallest at frequencies where the stress was weak. Little change in cross-shelf R_i^2 occurs at $\omega > 0.125$ cpd for all three models.

Consider now model L, which describes the variance due to local wind stress

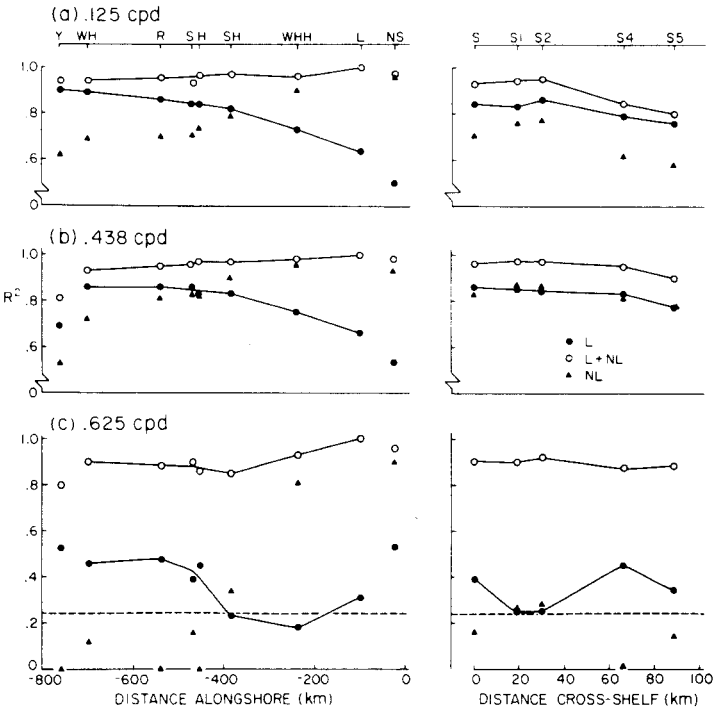

Fig. 12 Multiple coherence squared (R^2) attributed to models (4.1)–(4.3). Solid circles represent R_1^2, open circles represent R_2^2 and triangles represent R_3^2 at (a) 0.125, (b) 0.438 and (c) 0.625 cpd. The 95% level of significance is 0.24.

forcing only (solid circles in Fig. 12). The model was most effective at frequencies having high stress variance. R_1^2 increased to the west at all frequencies, in contrast to R_3^2. This tendency was particularly evident at $\omega < 0.5$ cpd, which implies that SSP responded more coherently to local forcing at frequencies where the dynamical model is valid.

Finally, consider the variance explained by the model L + NL containing local and non-local effects (open circles in Fig. 12). R_2^2 values for this model were consistently high ($R_2^2 \geq 0.9$), decreasing only slightly at higher frequencies or with distance downstream. Cross-shelf values of R_2^2 also show the increased effectiveness of L + NL. The difference between the values represented by the open and solid circles (the solid lines in Fig. 12) demonstrates how much more effective L + NL was, compared with a model considering local wind stress effects alone.

This comparison dramatically demonstrates the importance of free-wave energy in the SSP field, especially east of Halifax and at higher frequencies where the wind energy was low. Non-local effects were particularly evident at 0.625 cpd, where R^2 values doubled and even tripled with the addition of SSP^{NL} as a variable.

The contrast with the poor correlation of model NL is striking. Coastal SSP correlation scales were small at higher frequencies, suggesting the total SSP signal

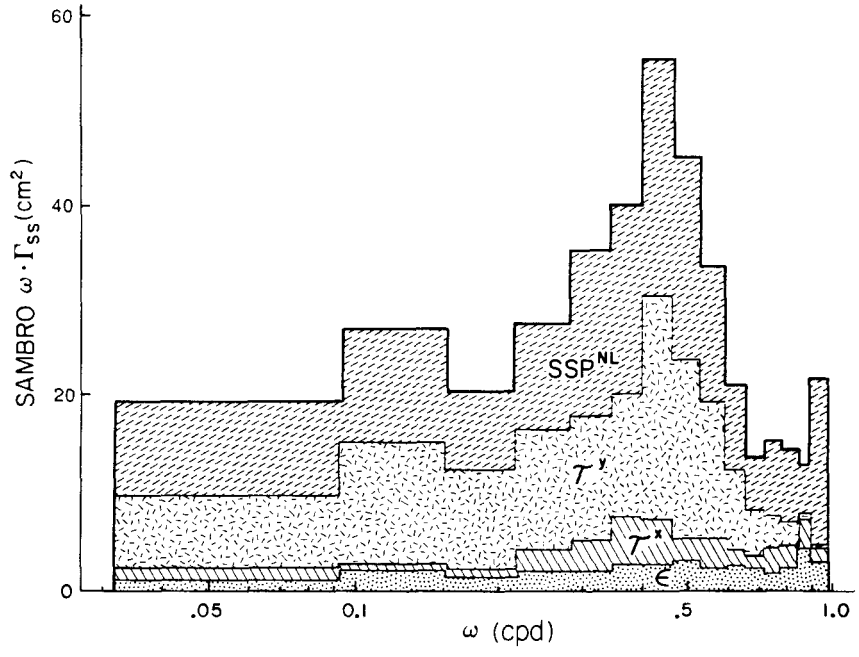

Fig. 13 Distribution of variance in Sambro SSP due to τ^y, τ^x and SSP^{NL} in model L + NL. Each level of shading represents the amount of variance due to each independent variable. The stipled area at the bottom denotes ϵ for the complete model.

was modified by local wind effects while the energy propagated downshelf. However, the residual SSP signal (i.e. after removal of wind effects) at all shelf positions was well correlated with the original free-wave signal at the eastern boundary of the Scotian Shelf, indicating that free energy travelled relatively unperturbed down the shelf. Local wind influences produced an evolution of, but did not necessarily dominate, the SSP field.

Figure 13 summarizes the frequency-dependent contributions of the three terms in L + NL at a representative SSP station (Sambro). The SSP variance in each frequency band is displayed in histogram form. Each region of shading represents the amount of variance attributed to each of the three independent variables. The figure demonstrates the nearly equal importance of local wind stress and non-local forcing at low frequencies ($\omega < 0.5$ cpd). The secondary role of τ^x is also seen. Finally note the increased importance of non-local forcing at higher frequencies ($\omega > 0.5$ cpd). Error in the complete model L + NL, represented by the stipled area under the histogram, is less than 10% of the total SSP variance. These results are generally applicable at all SSP locations, with non-local effects becoming more important at sites nearer the Laurentian Channel and slightly less important downstream of Sambro. However, it is important to note that the variance explained by the three terms described here remained essentially the same at all stations.

5 Discussion

Subtidal SSP variations during CASP are obviously dominated by two influences: local alongshelf wind stress and free-wave energy of a non-local, but possibly meteorological origin. How do these results compare with previous observations on the Scotian Shelf and on adjacent shelf regions? The results described here confirm other data suggesting the Scotian Shelf response is largely wind-driven (cf. Petrie and Smith, 1977; Smith et al., 1978; Sandstrom, 1980), but are incompatible with Sandstrom's data (1980) regarding free waves. An analysis of Sandstrom's data using a model with forced and free-wave contributions may produce different results.

These results are consistent with observations to the north and south as well. Observations from regions upstream of the Scotian Shelf are rather limited but SSP records from the central Labrador Shelf exhibit a distribution of variance with frequency similar to that shown here, and feature southward phase speeds highly suggestive of CTWs (J.F. Middleton, pers. comm.). Recent work by Wright et al. (1987) has provided a reasonable theory relating much of the Labrador Shelf SSP variability to atmospheric pressure-generated CTWs originating from Hudson Bay at 2–6 d periods. Thus free-wave energy from a very distant source apparently can propagate along the Labrador Shelf. The close visual agreement between the spectral responses of SSP off Labrador and Nova Scotia implies that free energy of a similar form, reinforced by local wind stress, can travel large distances and may reach the Scotian Shelf.

Subtidal wind and SSP energy west of the Scotian Shelf is concentrated at periods greater than 2.7 d, and SSP is highly coherent spatially and forced by meteorological transients (Beardsley et al., 1977). Cross-shelf variations in SSP variance on Nantucket Shoals, and the response to alongshelf stress (Brown et al., 1985), are very similar to those seen in the Halifax line. Noble and Butman (1979) analysed adjusted CSL and wind stress at several locations north of North Carolina, including Halifax and Eddy Point, N.S., near Whitehead Harbour. Many of their results agree with findings presented here. Sea-level and wind were spatially coherent at scales > 1200 km. The wind-driven response was almost exclusively due to alongshelf stress and increased from Eddy Point to Halifax. The amplitude of the Halifax SSP response to alongshelf stress was estimated to be 1 m Pa^{-1}. This response is similar in magnitude to that calculated in model L, where only local forcing was considered. However, it has been shown here that combining local and non-local terms in a statistical model substantially reduced the τ^y response. The range of 0.3–0.5 m Pa^{-1} found by Thompson (1986) using a regression model that considered local stress and non-local processes is more consistent with the values of $|\alpha_2|$ discussed here. Had Noble and Butman (1979) included some non-local effect in their calculations, a smaller estimate of the SSP response to alongshelf stress might have been obtained.

In a subsequent paper analysing the alongshelf current response in the Georges Bank and Middle Atlantic Bight regions, Noble et al. (1983) found 75–90% of the low-frequency (60–360 h) energy was due to combined wind-driven and free propagations. The transfer coefficient of alongshelf stress to current increased to the southwest, and a form of the arrested topographic wave model (Csanady, 1978) gave

good estimates of the observed current response. Phase speed estimates of free waves were similar to those reported here. Although the ratio of free to forced energy decreased in the free direction, the absolute free energy contribution increased in that direction as well, suggesting that CTWs are reinforced by incoherent wind stress fluctuations (i.e. non-linear transient wind responses over Georges Bank). Unfortunately their results were not separated into finer frequency bands.

The low-pass filtered SSP times series from the Labrador and Scotian Shelves exhibit a net phase speed in the free direction. It is much more difficult to discern free-wave propagations in the adjusted signals from the northern Middle Atlantic Bight. Noble and Butman (1979) and Wang (1979) observed southward (free) waves in the region south of Cape May. However, free waves in the north are masked by northward-directed forced waves. The resultant phase speeds north of Cape May suggest a combination of forced and free waves (Noble and Butman, 1979; Wang, 1979). Farther south in the South Atlantic Bight, the data are less uniform, but evidence for both types of forcing has been documented (Brooks, 1979; Schwing et al., 1988).

The combined effects of local alongshelf stress and distantly generated free waves are certainly the primary controlling factors of subtidal SSP along the entire east coast of North America. The relative importance of each factor depends very much on the geographic position, the frequency of the variations considered and even the time of year (Schwing et al., 1988). The similarity of the SSP response on the Scotian Shelf to those in the Labrador Shelf and Middle Atlantic Bight–Georges Bank regions suggests a continuum of meteorologically driven processes, with large-scale topographic effects (e.g. Laurentian Channel, Georges Bank) coming into play. However, small-scale topographic features, like those on the Scotian Shelf, do not appear to be a major impediment to subtidal SSP variability.

These results have at least one other important implication for modelling strategies. In addition to suggesting appropriate model types to explain the physics behind the forced and free responses of the Scotian Shelf, the relationship of the transfer functions provides information to evaluate proper upshelf boundary conditions (i.e. Laurentian Channel) for Scotian Shelf models. The interpretation of these results can also be used to infer upshelf boundary conditions for Gulf of Maine models. Although they are not precisely known, Wright et al. (1986) have shown that proper conditions are necessary to achieve accurate "steady-state" model results.

6 Summary

Subtidal SSP on the inner portion of the Scotian Shelf is controlled by two primary forces – local alongshelf wind stress and non-locally generated free wave energy. Cross-shelf stress is of only minor importance. Together these terms explain more than 90% of all SSP variance. However, the relative importance of these factors depends on geographical position and frequency.

The response of SSP to local forcing exhibits the features of a dynamical model forced by a time-dependent alongshelf wind stress and clamped at the upshelf boundary. SSP is most coherent with τ^y, and the response amplitude increases with distance downshelf. The signal also propagates in the free direction. Cross-shelf coherence and amplitude decrease, and phase propagates offshore.

The free response decreases in coherence and amplitude with distance offshore and away from its upshelf source, much like a classic CTW (Gill and Schumann, 1974). It is observed at all frequencies, but the relative contribution of non-local energy to the SSP signal is greatest at frequencies where the stress is weak. The effectiveness of non-local forcing also is greater at locations nearer Cabot Strait. Phase speeds along the coast are consistent with first and second mode CTWs. These results provide the most direct evidence of CTW on the Scotian Shelf to date, and imply that the Laurentian Channel does not completely block free-wave energy from propagating downstream.

A substantial change in the statistically estimated response to τ^y is observed when the non-local contribution to SSP is ignored. This disparity is greatest at frequencies with the highest wind variance. The response to τ^y in the complete model compares more favourably with that in the dynamical solution. Thus a statistical model considering both local wind stress and free waves of a non-local origin is a more physically reasonable representation of SSP dynamics.

Acknowledgements

I am grateful to several individuals for their stimulating scientific discussion and critical review during the preparation of this manuscript, most notably Drs Keith Thompson, Peter Smith, Dan Wright and Carl Anderson. I also thank Jackie Hurst for TEXing this paper. This work was supported (in part) by the Federal Panel on Energy R & D (PERD).

References

BEARDSLEY, R.C.; H. MOFJELD, M. WIMBUSH, C.N. FLAGG and J.A. VERMERSCH, JR. 1977. Ocean tides and weather-induced bottom pressure fluctuations in the Middle-Atlantic Bight. *J. Geophys. Res.* **82**: 3175–3182.

BROOKS, D.A. 1979. Coupling of the Middle and South Atlantic Bights by forced sea level oscillations. *J. Phys. Oceanogr.* **9**: 1304–1311.

BROWN, W.S.; N.R. PETTIGREW and J.D. IRISH. 1985. The Nantucket Shoals Flux Experiment (NFSE79). Part II: The structure and variability of across-shelf pressure gradients. *J. Phys. Oceanogr.* **15**: 749–771.

CARTER, G.C. and J.F. FERRIE. 1979. A coherence and cross-spectral estimation program. *In*: Programs for digital signal processing. Edited by the Digital Signal Processing Committee, IEEE Acoust, Speech and Signal Processing Soc, IEEE New York, pp. 2.3.1–2.3.18.

CSANADY, G.T. 1978. The arrested topographic wave. *J. Phys. Oceanogr.* **8**: 47–62.

DRINKWATER, K.; B. PETRIE and W.H. SUTCLIFFE, JR. 1979. Seasonal geostrophic volume transports along the Scotian Shelf. *Estuar. Coastal Mar. Sci.* **9**: 17–27.

FREELAND, H.J.; F.M. BOLAND, J.A. CHURCH, A.J. CLARKE, A.M.G. FORBES, A. HUYER, R.L. SMITH, R.O.R.Y. THOMPSON and N.J. WHITE. 1986. The Australian Coastal Experiment: A search for coastal-trapped waves. *J. Phys. Oceanogr.* **16**: 1230–1249.

GARRETT, C. and B. TOULANY. 1982. Sea level variability due to meteorological forcing in the northeast Gulf of St. Lawrence. *J. Geophys. Res.* **87**: 1968–1978.

GILL, A.E. and E.H. SCHUMANN. 1974. The generation of long shelf waves by the wind. *J. Phys. Oceanogr.* **4**: 83–90.

HUTHNANCE, J.M. 1981. Waves and currents near the continental shelf edge. *Prog. Oceanogr.* **10**: 193–226.

JENKINS, G.M. and D.G. WATTS. 1968. *Spectral Analysis and Its Applications*. Holden-Day, Oakland, Calif., 525 pp.

LIVELY, R.R. 1987. Current meter, meteorological, sea-level and hydrographic observations from the CASP Experiment, off the coast of Nova Scotia, November 1985 to April 1986. Can. Tech. Rep. Hydrogr. Ocean Sci., vii + 454 pp.

NOBLE, M. and B. BUTMAN. 1979. Low-frequency wind-induced sea level oscillations along the east coast of North America. *J. Geophys. Res.* **84**: 3227–3236.

NOBLE, M.; B. BUTMAN and E. WILLIAMS. 1983. On the longshore structure and dynamics of subtidal currents on the eastern United States continental shelf. *J. Phys. Oceanogr.* **13**: 2125–2147.

PETRIE, B.D. 1983. Current response at the shelf break to transient wind forcing. *J. Geophys. Res.* **88**: 9567–9578.

PETRIE, B.D. and P.C. SMITH. 1977. Low-frequency motions on the Scotian Shelf and Slope. *Atmosphere*, **15**: 117–140.

SANDSTROM, H. 1980. On the wind-induced sea level changes on the Scotian Shelf. *J. Geophys. Res.* **85**: 461–468.

SCHWING, F.B.; L.-Y. OEY and J.O. BLANTON. 1988. Evidence for non-local forcing along the southeastern U.S. during a transitional wind regime. *J. Geophys. Res.*, **93**: 8221–8228.

SMITH, S.D. and E.G. BANKE. 1975. Variation of the sea surface drag coefficient with wind speed. *Q.J.R. Meteorol. Soc.* **101**: 665–673.

SMITH, P.C. and B.D. PETRIE. 1982. Low-frequency circulation at the edge of the Scotian Shelf. *J. Phys. Oceanogr.* **12**: 28–46.

———; ——— and C.R. MANN. 1978. Circulation variability, and dynamics of the Scotian Shelf and Slope. *J. Fish. Res. Board Can.* **35**: 1067–1083.

THOMPSON, K.R. 1986. North Atlantic sea-level and circulation. *Geophys. J.R. Astronom. Soc.* **87**: 15–32.

WANG, D.-P. 1979. Low frequency sea level variability on the Middle Atlantic Bight. *J. Mar. Res.* **37**: 683–697.

WRIGHT, D.G. 1986. On quasi-steady shelf circulation driven by along-shelf wind stress and open-ocean pressure gradients. *J. Phys. Oceanogr.* **16**: 1712–1714.

———; D.A. GREENBERG, J.W. LODER and P.C. SMITH. 1986. The steady-state barotropic response of the Gulf of Maine and adjacent regions to surface wind stress. *J. Phys. Oceanogr.* **16**: 947–966.

———; ——— and F.G. MAJAESS. 1987. The influence of bays on adjusted sea level over adjacent shelves with application to the Labrador Shelf. *J. Geophys. Res.* **92**: 14,610–14,620.